Catalysis Science & Technology

Accepted Manuscript

ROYAL SOCIETY OF CHEMISTRY

www.rsc.org/catalysis

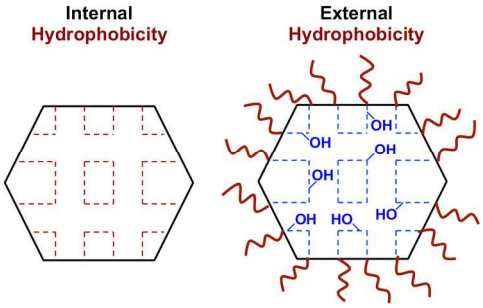

Microporous and mesoporous silicates with internal or external hydrophobic surfaces show differences in catalytic reactivity and stability in liquid water.

Hydrophobic Microporous and Mesoporous Oxides as Brønsted and Lewis Acid Catalysts for Biomass Conversion in Liquid Water

Rajamani Gounder*

School of Chemical Engineering, Purdue University, 480 Stadium Mall Drive, West Lafayette, IN 47907, USA

*Corresponding author. E-mail: rgounder@purdue.edu

Abstract

The use of heterogeneous catalysts in liquid water, even at the moderate temperatures (<523 K) typical of most condensed-phase biomass conversion processes, is often fraught with issues related to structural instability and to active site inhibition or deactivation by mechanisms that differ from those prevalent in the gas phase at higher temperatures. One strategy to address these issues in porous silica-based oxides is to design or functionalize their surfaces with hydrophobic structures or domains. Hydrophobic moieties can be present either at external crystallite surfaces or within the internal porous voids where most active sites typically reside. Both extracrystalline and intracrystalline hydrophobic environments can prevent the condensation of bulk water within internal void spaces and thus alleviate any transport restrictions its presence may cause, while only intracrystalline environments can influence the kinetic effects of molecular water at active sites. As a result, hydrophobic environments at external and internal crystallite surfaces can have fundamentally different consequences for reactivity, in spite of the phenomenological similarities of their effects on observed reaction rates. The conceptual distinction between these two forms of hydrophobicity, together with accurate assessments of transport and kinetic contributions to measured reaction rates, can inform the placement of hydrophobic domains at appropriate locations in porous solids to cause predictable changes in reactivity. This mini-review discusses these concepts within the context of recent studies that have used hydrophobic Brønsted and Lewis acidic microporous and mesoporous oxides in catalytic reactions of biomass-derived molecules in liquid water and biphasic water-organic mixtures.

1. Introduction

Lignocellulosic biomass is a renewable and nearly carbon-neutral feedstock that can partially replace fossil carbon resources used in the synthesis of transportation fuels and chemicals.[1] Thermal and chemical routes can convert biomass feedstocks into a wide variety of chemical intermediates including synthesis gas (via gasification), a diverse mixture of organic compounds known as "bio-oil" (via pyrolysis), and the carbohydrate and aromatic constituents of cellulose, hemicellulose, and lignin (via hydrolysis).[2] Chemical intermediates derived from pyrolysis and hydrolysis routes are highly functional and highly oxygenated, and their upgrading into useful chemical or fuel compounds often involves reaction networks with multiple steps that form carbon-carbon bonds, remove oxygen atoms, and add hydrogen.[2] In this context, Brønsted and Lewis acids catalyze useful reactions such as esterification, condensation, dehydration, and transfer hydrogenation.[3-6] They have been used to do so in sequential reaction networks, as in the conversion of cellulose-derived glucose into 5-hydroxymethylfurfural (HMF) via Lewis acid-catalyzed glucose-fructose isomerization and Brønsted acid-catalyzed fructose dehydration to HMF (Scheme 1).[7] A diverse range of liquid solvents have been investigated in processes to upgrade pyrolysis-derived organic compounds and hydrolysis-derived sugar monomers, including water, organic media (e.g., alkylphenols[8, 9], gamma-valerolactone[10-12]) and ionic liquids.[13, 14] The use of solid acid catalysts and liquid solvents in condensed-phase biomass conversion routes presents technical challenges in the development of heterogeneous catalysts that maintain their reactivity and structure during reaction.

Heterogeneous Brønsted and Lewis acidic oxide catalysts with hydrophobic surface properties have emerged recently as a class of materials that offer improved resistance to deactivation mechanisms that prevail during biomass conversion in liquid water and biphasic

water-organic mixtures.[15-17] In liquid water, solid oxides can deactivate because of irreversible structural changes and degradation, or because of reversible inhibition of active catalytic centers by adsorbed or co-adsorbed solvent molecules. Silica surfaces in microporous molecular sieves,[18, 19] ordered mesoporous materials[20-22] and amorphous networks enforce multiple-point coordination of metal (M) heteroatoms by lattice oxygen atoms that helps prevent hydrolysis and leaching. Hydrophobic domains in silica surfaces disrupt the formation of extended water phases near them and further mitigate Si-O-Si and Si-O-M bond hydrolysis events that cause active site decomposition in aqueous media. Hydrophobic surroundings near active sites also cause the weaker binding of water at such sites, which helps attenuate catalytic inhibition caused by competitive adsorption. Thus, the extended oxide networks and hydrophobic environments found in solid Brønsted and Lewis acidic oxides confers structural stability that is seldom found in homogeneous acids in liquid water,[23] and generally leads to observed enhancements in reactivity for hydrophobic solids.

This mini-review provides an abridged survey of recent reports in the synthesis of Brønsted and Lewis acidic microporous and mesoporous silica-based oxides with hydrophobic properties, and their applications for biomass conversion in water or biphasic water-organic mixtures. Specific examples are chosen that illustrate issues noted broadly regarding the stability of solid oxide catalysts in liquid water, and that reflect findings reported generally regarding the observed catalytic effects of hydrophobic surfaces or moieties in Brønsted and Lewis acidic solids. A conceptual distinction is drawn between hydrophobic environments within internal micropore and mesopore surfaces (Scheme 2a) and at external crystallite surfaces (Scheme 2c, 2d), because they can have fundamentally different catalytic consequences, even when their effects on observed reaction rates appear similar. Finally, a brief outlook is provided for future

research opportunities in the synthesis and applications of hydrophobic Brønsted and Lewis acidic oxides for biomass conversion.

2. Brønsted and Lewis acid sites in hydrophobic oxides

Experimental studies have shown that the non-polar Si-O-Si connectivities comprising purely siliceous surfaces are hydrophobic and do not adsorb water,[24] yet hydroxyl groups located at defect sites (e.g., Si-OH)[24] and framework heteroatoms (e.g., Si-O(H)-Al)[25] are hydrophilic and adsorb water molecules and clusters. In the case of microporous materials, mordenite zeolites of varying Si/Al ratio (~80–200), prepared by framework Al extraction and vacancy defect healing, adsorbed water (298 K) in amounts that correlated linearly with Al content.[25] Similar observations have been reported for mesoporous materials, in which the grafting of chlorotrimethylsilane onto defect Si-OH groups in MCM-41 led to a decrease in water uptakes (298 K).[26] Combined calorimetric and gravimetric measurements have shown that water can adsorb on isolated framework Ti^{4+} centers in highly defective and low-defect beta zeolites (Ti-Beta), but with more negative adsorption enthalpies at Ti sites isolated within highly defective Ti-Beta.[27] These more negative adsorption enthalpies reflect the additional stabilization of bound water molecules provided by hydrogen bonding interactions with hydroxyl groups proximal to Ti sites in highly defective zeolites.[27] In fact, the higher density of defect silanol groups in Ti-Beta zeolites crystallized in hydroxide media (Scheme 2b) leads to water uptakes that are significantly higher (by >30x at P/P_0 = 0.2, 293 K, Figure 1) than on low-defect Ti-Beta zeolites crystallized in fluoride media (Scheme 2a), whose micropores are unable to condense water at ambient pressures.[15] ^{119}Sn magic angle spinning nuclear magnetic resonance (MAS NMR) spectroscopy detects isolated framework Sn^{4+} centers as octahedrally-coordinated species in low-defect zeolite

beta (Sn-Beta) exposed to ambient conditions, but instead as tetrahedrally-coordinated species after dehydration treatments (vacuum at 393 K), indicating that framework Sn sites coordinate with two water molecules even when confined within hydrophobic zeolite micropores.[28]

Theoretical studies have reported findings consistent with experiment regarding the adsorption behavior of water on hydrophilic binding sites located in hydrophobic surfaces. Molecular dynamics simulations by Giovambattista et al. indicate that liquid-phase water is not stable between hydrophobic surfaces separated by less than ~0.80 nm (at ambient pressures),[29] but individual water molecules can adsorb at hydrophilic silanol defects isolated within hydrophobic silica surfaces.[30] Similarly, molecular dynamics simulations of water adsorption on hydrophobic talc surfaces by Rotenberg et al. indicate that water adsorbs at hydrophilic binding sites in surfaces that are not wetted by liquid water.[31] These findings, in turn, imply that water molecules can adsorb at hydrophilic binding sites within hydrophobic zeolite micropores below pressures required for the intrusion of liquid water.[31] Configurational bias Monte Carlo simulations also show that bulk water is excluded from defect-free micropores in Si-Beta at ambient pressures.[32] In fact, the release of water molecules from glucose hydration spheres in solution provides the entropic driving force required for glucose adsorption into hydrophobic micropores.[32]

These experimental and theoretical studies indicate that trivalent heteroatoms (e.g., Al^{3+}) that generate Brønsted acidic hydroxyl groups and tetravalent heteroatoms (e.g., Sn^{4+}, Ti^{4+}) that generate Lewis acidic centers in siliceous frameworks behave as hydrophilic binding sites for water, even when they are located within hydrophobic surrounding environments. Microporous silicates with defect-free internal surfaces are hydrophobic and, in the presence of bulk water, will prevent internal micropore condensation of water. In contrast, siliceous surfaces containing

defect silanol groups, whether located at external crystallite surfaces or defective internal porous voids, are covered by or filled with water in the presence of liquid water. As is discussed next, the presence or absence of liquid-phase water within internal voids can have dramatic consequences for the structural stability of porous silicates in aqueous media.

3. Stability of microporous and mesoporous silicates in aqueous media

Brønsted acidic zeolites are used widely in the petrochemical industry as catalysts for gas-phase reactions of hydrocarbons at elevated temperatures (>523 K),[18, 33, 34] in which issues of hydrothermal stability predominantly reflect steam-catalyzed cleavage of framework Al-O bonds that leads to dealumination (Scheme 3).[35, 36] In contrast, the structural stability of Brønsted acidic zeolites is compromised in liquid water at even the moderate temperatures (<523 K) used typically for condensed-phase reactions of biomass-derived oxygenates.[37, 38] For example, H-form zeolites (e.g., H-MFI, H-BEA, H-USY) remain stable while catalyzing the dehydration of alcohols (methanol,[39-41] ethanol,[42] 2-butanol[43]) in the gas phase (343-433 K), but not while catalyzing the dehydration of 2-butanol in hot liquid water (513 K).[44] After contacting H-form zeolites with hot liquid water for up to 6 hours (423-473 K), Ravenelle et al. did not observe any structural changes to H-MFI zeolites but reported losses in the crystallinity of H-FAU zeolites that became more severe with increasing contact time, indicating that the hydrothermal stability of zeolites depends on the framework topology.[45] H-FAU zeolites showed greater losses in crystallinity as their Si/Al ratio increased (5-41),[45] suggesting that the predominant mechanism for water-catalyzed structural degradation of aluminosilicate zeolites involves the hydroxide-catalyzed cleavage of framework siloxane (Si-O-Si) bonds (Scheme 3). Kruger et al.[46, 47] showed that under the more acidic conditions (pH ~3) used for fructose dehydration to HMF in aqueous

media (403 K), H-zeolites (e.g., H-BEA, H-FAU) undergo partial dissolution to form soluble aluminosilicate species that catalyze undesired side reactions of HMF that form levulinic acid, formic acid and polymeric humins.[43, 44] Taken together, these studies indicate that large-pore aluminosilicate zeolites (FAU, BEA) are structurally unstable in hot liquid water (403-473 K), with hydroxide-mediated Si-O-Si hydrolysis predominant in nearly neutral media (pH ~6-7) and Si-O-Al hydrolysis predominant in acidic media (pH ~3).

Consistent with these reports, Zapata et al. observed that H-FAU zeolites with highly-defective and hydrophilic external crystallite surfaces (Scheme 2b) underwent nearly complete structural degradation after 3 hours in hot liquid water (473 K), as detected by X-ray diffraction, scanning electron microscopy, and N_2 micropore volumes (>95% decrease).[48, 49] Functionalization of H-FAU zeolites with organosilanes of different alkyl chain length (C_2-C_{18}) decreased OH vibrational band intensities in DRIFTS spectra for silanol groups at external crystallite surfaces and, to a lesser extent, for Brønsted acidic hydroxyl groups located within internal microporous voids.[48, 49] Organosilane functionalization, which occurred predominantly at external H-FAU surfaces, made crystallites very hydrophobic and led to dramatic improvements in their stability in hot liquid water and in two-phase water-decalin emulsions (473 K, 0-22 hours).[48, 49] These authors concluded that organosilane functionalization prevented contact of internal porous voids with liquid water, which otherwise causes irreversible structural degradation via hydrolysis reactions and the subsequent solvation and transport of zeolitic fragments into the extracrystalline liquid phase.[48] Hydrothermal treatments of H-FAU zeolites with an equivalent chemical potential of water in the vapor phase (473 K) did not lead to structural collapse, indicating that rates of crystallite fragment dissolution and transport into bulk solution, and not rates of framework hydrolysis, were responsible for the structural degradation

observed in hot liquid water.[49] Conceptually, the steps involved in zeolite dissolution in aqueous media are analogous to those involved in zeolite recrystallization.[50]

Ordered mesoporous silicas, by virtue of their chemical composition, are also subject to issues related to the low hydrothermal stability of siloxane bonds in hot liquid water.[20, 22] Pollock et al. used N_2 adsorption, X-ray diffraction and small angle neutron scattering to observe that structural degradation of pure-silica SBA-15 occurred more rapidly when treated hydrothermally in liquid water than in water vapor (388-428 K).[51] These authors proposed that faster transport rates of soluble $Si(OH)_4$ species in liquid water led to their preferential re-deposition in voids smaller than the primary mesopores.[51] The incorporation of larger amounts of Al atoms in MCM-41[52-54] and MCM-48[52, 55] frameworks also increased their hydrothermal stability in hot liquid water (373 K), consistent with hydrolysis mechanisms that selectively target framework siloxane bonds in microporous materials (Scheme 3).[45] These studies indicate that the effects of solid-liquid water contact and of Al content in solid oxide frameworks on structural stability are similar for both mesoporous and microporous silicates.

The incorporation of organic functional groups into ordered mesoporous materials imparts hydrophobic character to mesopore surfaces, reflected in lower intrapore water concentrations measured using thermogravimetric analysis methods.[56, 57] MCM-41 materials functionalized with methyl, ethyl, and phenyl groups were structurally more stable than pure-silica MCM-41 when exposed to ambient conditions (10 months) or to boiling liquid water (373 K, 8 hours), suggesting that siloxane hydrolysis rates were lower within more hydrophobic mesopores that contained lower water content.[57] Certain organic functional groups (e.g., sulfonic acids) also incorporate Brønsted acid sites into mesoporous silicas, in which additional deactivation mechanisms involve water-catalyzed cleavage of functional groups from the silica

surface. The stability of propylsulfonic acid groups on SBA-15 materials may be improved by increasing the number of attachments to mesopore surfaces, as occurs via co-condensation during synthesis relative to post-synthetic grafting.[58] Tucker et al.[59] reported that incorporating additional hydrophobic ethyl functional groups into the mesopores of propylsulfonic acid-functionalized SBA-15 materials led to less severe deactivation during catalytic dehydration of fructose to HMF (403 K, 4:1 THF:H_2O solvent mixture), ascribing these effects to lower intrapore water concentrations and, in turn, lower hydrolysis rates of the active propylsulfonic acid sites.

4. Catalysis with hydrophobic microporous materials

4.1. Brønsted acidic microporous silicates

Hydrophobic zeolites have been used to describe a class of microporous materials whose external crystallite surfaces have been functionalized with hydrophobic moieties (Scheme 2d), and a distinctly different class of microporous materials whose internal surfaces are sufficiently hydrophobic to prevent the condensation of liquid water within them under ambient conditions (Scheme 2a). The external functionalization of crystallites creates hydrophobic particles whose surfaces are not wetted by water, causing them physically segregate in organic phases of biphasic mixtures.[49] Zapata et al. studied Brønsted acid-catalyzed alkylation of *m*-cresol with 2-propanol in liquid water (473 K) and showed that the hydrophobic nature of organosilane-functionalized H-USY prevented liquid water from accessing internal pore spaces, but did not prevent vapor-phase water from adsorbing at Brønsted acidic protons located within these pores.[48, 49] Water molecules adsorbed at active sites within porous voids that are in chemical equilibrium with liquid water in extracrystalline phases have an equivalent chemical potential, and thus provide an

equivalent driving force for chemical reactions.[49, 60] As a result, zeolites whose external surfaces are functionalized by hydrophobic groups but whose internal voids otherwise are identical (Scheme 2b and 2d) will show differences in observed reaction rates or structural stability that depends on transport rates of molecules to or from active sites in internal void spaces, but not if limited by kinetic events that occur at active sites.[60]

Glucose acetalization reactions with *n*-butanol to form butyl glucosides were investigated by Camblor et al. on two series of H-BEA samples of varying Si/Al ratio, one that was essentially free of siloxane connectivity defects and another that contained a high density of internal and external silanol defects because of treatments with nitric acid.[61] Within each series of H-BEA samples, the addition of more Al atoms increased both the number (per g) of H^+ sites and the amount of adsorbed water measured by thermogravimetric methods (weight losses below 523 K).[61] Initial rates of glucose acetalization (per g, 393 K) increased with Al content and the number of H^+ sites, but only up to a point, after which rates (per g) decreased with increasing Al content as the samples became more hydrophilic. The Si/Al ratio corresponding to the highest acetalization rate (per g) within each series was lower for the low-defect and more hydrophobic H-BEA series (Si/Al = 29) than for the highly defective H-BEA series (Si/Al = 118).[61] From these data, these authors proposed that initial glucose acetalization rates (per g) depended both on the number of active H^+ sites that catalyze the acetalization reaction, and the hydrophobic nature of internal voids that influences the intrazeolitic adsorption and transport rates of n-butanol reactants.[61]

More recently, Arias et al. studied the etherification of 5-hydroxymethylfurfural (HMF) with alcohols over Brønsted acidic zeolites to form 5-alkoxymethylfurfural intermediates, and their subsequent oxidation over gold particles supported on ceria to form the corresponding

furoic compounds.[62] The desired condensation intermediates are formed from cross-etherification of HMF with *n*-octanol, while undesired intermediates are formed from HMF self-etherification reactions that become more prevalent with increasing HMF concentration. Among a series of aluminosilicate H-BEA samples of varying Si/Al ratio (12-100), the selectivity toward HMF-*n*-octanol cross-etherification (373 K) increased systematically (~2-47) with increasing Si/Al ratio as H-BEA zeolites became more hydrophobic.[61] The selectivity toward HMF-*n*-octanol cross-etherification was also higher on H-BEA than on the more hydrophilic H-USY material studied.[61] These selectivity dependences on Si/Al ratio and zeolite topology were proposed to reflect a stronger preference for the adsorption of less polar *n*-octanol, over more polar HMF, as pore environments became more hydrophobic.[61]

4.2. Lewis acidic microporous silicates

Hydrophobic MFI molecular sieves containing isolated framework Lewis acidic Ti^{4+} sites (TS-1) were the first materials discovered to activate H_2O_2 as an oxidant in aqueous media.[63, 64] Their catalytic predecessors were hydrophilic, amorphous mixed titania-silica catalysts that maintained reactivity in organic hydroperoxides and anhydrous H_2O_2, but not in aqueous H_2O_2.[65] Khouw et al. reported nearly identical conversions for 1-hexene epoxidation (323 K) and *n*-octane oxidation (353 K) with hydrophobic TS-1 in both aqueous and anhydrous H_2O_2 (Table 1), but conversions with hydrophilic TiO_2–SiO_2 that were one order-of magnitude higher in anhydrous H_2O_2 than aqueous H_2O_2 (Table 1).[65] In aqueous H_2O_2, conversions for *n*-octane oxidation and 1-hexene epoxidation were higher by >29x and >100x, respectively, on hydrophobic TS-1 than on hydrophilic TiO_2-SiO_2 (Table 1).[65] The discovery of hydrophobic TS-1 zeolites enabled replacing amorphous mixed TiO_2–SiO_2 catalysts for hydrocarbon oxidation

processes,[66] and opened new opportunities to mediate selective oxidation reactions using solid Lewis acids in liquid water.[5, 66]

Hydrophobic beta zeolites containing isolated framework Lewis acidic Sn^{4+} and Ti^{4+} centers were recently reported to isomerize cellulose-derived glucose into fructose[67] and hemicellulose-derived xylose into xylulose[68] in liquid water (363-413 K), via intramolecular Meerwein-Ponndorf-Verley reduction and Oppenauer oxidation (MPVO) reaction mechanisms.[69] The catalytic consequences of hydrophobic environments surrounding Ti centers were studied by comparing low-defect and hydrophobic Ti-Beta zeolites crystallized in fluoride media, highly-defective and hydrophilic Ti-Beta zeolites crystallized in hydroxide media, and hydrophilic amorphous TiO_2–SiO_2 materials.[70] Glucose isomerization rate constants (per total Ti, 373 K) in liquid water, measured in the absence of internal mass transfer limitations, were higher (by >10x, Table 1) on hydrophobic Ti-Beta zeolites than on hydrophilic TiO_2-SiO_2.[70] Interpretation of these rate constants using a mechanism-derived rate expression indicated that higher rate constants on hydrophobic zeolites reflected, in part, the weaker inhibition of Ti sites by competitively-adsorbed water molecules that were the kinetically-relevant and most abundant surface intermediates.[70] Similar observations were reported by Corma et al. upon silylation of Sn-Beta zeolites with hexamethyldisilazane to form more hydrophobic materials, which showed order-of-magnitude higher turnover rates for intermolecular MPVO reactions between cyclohexanone and 2-butanol (373 K) with 10% water in the reaction medium.[71]

5. Catalysis with hydrophobic mesoporous materials

5.1. Brønsted acidic mesoporous silicates

Recent attention has focused on applications of Brønsted acidic mesoporous silicas to catalyze the dehydration of hydrolysis-derived sugars to furans.[58, 72, 73] Crisci et al. functionalized SBA-15 materials with either 3-(propylthio)propane-1-sulfonic acid groups or propylsulfonic acid groups and studied them for fructose dehydration to HMF in biphasic aqueous-organic mixtures (403 K).[73] Higher fructose conversions and selectivities to HMF were observed on the 3-(propylthio)propane-1-sulfonic acid-functionalized material, which the authors speculated might have resulted from the more hydrophobic nature of these functional groups.[73] Alamillo et al. used a polar aprotic polymer (poly(vinylpyrrolidine)) to further functionalize the internal mesopores of propylsulfonic acid-functionalized SBA-15, and observed an enrichment in the furanose tautomer among the distribution of adsorbed and confined fructose molecules, relative to its proportion found within the tautomer distribution in unmodified SBA-15.[72] In turn, this enrichment led to a higher selectivity to HMF because the furanose tautomer of fructose is the preferred precursor to form HMF via dehydration.[72] These studies demonstrate that both the rates and selectivities of fructose dehydration reactions can be influenced by the solvating environments present within solid mesoporous silicas, in a manner reminiscent of the rate and selectivity differences that result from differences among liquid solvents.

Brønsted acidic mesoporous silicas have also been studied for the esterification of pyrolysis-derived carboxylic acids with alcohols.[74-76] Miao et al. measured initial rates of acetic acid esterification with methanol (323-343 K) on SBA-15 materials modified with sulfonic acid and propylsulfonic acid groups.[75] Although esterification rate constants decreased on both materials as the water content increased in the reactant mixture, this inhibition by water was attenuated for the propylsulfonic acid-modified SBA-15 material, suggesting that the hydrophobic propyl groups linked covalently to Brønsted acidic sulfonic acid centers may have

helped mitigate the inhibitory effects of water.[75] Further experiments were performed to incorporate additional propyl groups into the surfaces of sulfonic acid-modified SBA-15, both during and after synthesis of the material.[75] These treatments led to materials that showed attenuated inhibition of initial esterification rates by water, relative to unmodified sulfonic acid-SBA-15.[75] Taken together, these findings indicate that hydrophobic functional groups located near Brønsted acidic sulfonic acid groups in mesoporous SBA-15 materials help mitigate inhibition or deactivation in liquid water.

5.2. Lewis acidic mesoporous silicates

Lewis acidic mesoporous silicates can show higher reactivity than their microporous analogs when reaction rates are limited by diffusion or access to active sites, as occurs for glucose isomerization in MFI zeolites,[67] whose micropores are much smaller in diameter (~0.55 nm) than glucose reactants (~0.7-0.8 nm). Recently, Dapsens et al. prepared hierarchical Sn-MFI zeolites by alkaline treatment of Sn-MFI and by alkaline-assisted insertion of Sn atoms into Si-MFI frameworks.[77] Hierarchical Sn-MFI zeolites containing mesopores or Sn atoms near external crystallite surfaces showed detectable glucose conversions to fructose (353 K), while microporous Sn-MFI samples were unable to convert glucose.[77] In contrast, Lewis acidic mesoporous silicates such as Ti-MCM-41 and Sn-MCM-41 have been reported to catalyze glucose-fructose isomerization in liquid water, but with conversions lower (by ~2.5x, 413 K, Table 2) than their large-pore (~0.70 nm diameter) molecular sieve Ti-Beta and Sn-Beta analogs.[67] One plausible explanation of the lower conversions observed on Lewis acidic mesoporous materials than on Beta molecular sieves (Table 2), in the absence of mass transfer limitations, may reflect the more hydrophilic pore environments found within defective

mesoporous structures, given that water inhibits glucose isomerization turnovers at Lewis acid sites.[70]

Methods to graft organosilane compounds onto internal silanol groups of mesoporous titanosilicates, which increased their hydrophobicity and reactivity for aqueous-phase alkene epoxidation reactions, were reported in pioneering studies by the Tatsumi and Corma groups.[78-80] Additional information on the design and synthesis of microporous and mesoporous titanosilicates with desired structural, textural, and hydrophobic properties can be found in an extensive review published recently by Moliner and Corma.[81] Although post-synthetic grafting of organic or inorganic moieties onto hydroxyl groups is a versatile method to functionalize mesoporous silicates, such methods can, in certain cases, also cause unintended structural modification to catalytic active sites. For example, turnover numbers (per total Ti) for cyclooctene epoxidation in aqueous H_2O_2 (343 K) increased as more hydrophobic triethoxyfluorosilane groups were grafted in Ti-SBA-15 mesopores, but only up to a point, after which turnover numbers decreased with increasing silane content as functional groups began blocking active Ti centers.[82] Similarly, post-synthetic grafting of organosilanes onto silanol defects in microporous silicates can also result in grafting onto Brønsted acidic hydroxyl groups, as reported by Zapata et al. on H-FAU zeolites.[48, 49]

One example studied recently in the area of biomass conversion have been reactions of glycerol, a byproduct of biodiesel production from triglycerides, via acetalization with acetone to form solketal on Lewis acidic mesoporous materials (Zr-TUD-1, Hf-TUD-1, Sn-MCM-41).[83] Li et al. reported that glycerol conversion (353 K) and turnover frequencies (per total Lewis and Brønsted acid site) were higher on Zr-TUD-1 and Hf-TUD-1 than on Al-TUD-1.[83] Water uptakes quantified by thermogravimetric analysis indicated that Zr- and Hf-TUD-1 adsorbed lower

amounts of water (by at least 2-3x, per nm^2) than Al-TUD-1, and was used as evidence to support the proposal that more hydrophobic pores facilitated the transport of water products away from active sites to mitigate reversible solketal hydrolysis.[83] Similar proposals for the role of hydrophobic pore environments in Brønsted acidic aluminosilicate H-BEA zeolites for glycerol acetalization were also reported by da Silva et al.[84] Collectively, the examples discussed in Sections 4 and 5 illustrate that the hydrophobicity of microporous and mesoporous silicates influence observed reactivity and selectivity for catalytic reactions in liquid water, but for different underlying reasons. In the final section, conclusions regarding the influence of hydrophobicity on catalytic reactivity are provided together with an outlook for further opportunities in this emerging research area.

6. Conclusions and Outlook

This mini-review highlights several examples in which hydrophobic porous materials show higher reactivity than their hydrophilic analogs in liquid water, even if the origin of such reactivity enhancements reflect different underlying phenomena. Catalytic reactions of biomass-derived molecules on porous solids in liquid water, and heterogeneously-catalyzed reactions by porous solids in general, involve coupled reaction-transport phenomena.[85] The hydrophobic functionalization of external zeolite crystallite surfaces can prevent bulk water from entering internal void spaces, but molecular water can still adsorb within pores and with an equivalent chemical potential as bulk water under conditions of chemical equilibrium.[49] As a result, the functionalization of external crystallite surfaces can only influence initial or steady-state catalytic rates that depend on diffusion or transport rates, but not on events of kinetic origin.[60] In contrast, internal hydrophobic micropore surfaces can prevent bulk water from filling void spaces while

also changing the environment around active sites and, in turn, the solvation and binding of reactants and solvent molecules at these sites.[27, 70] Thus, internal hydrophobic voids can influence observed rates of catalytic processes that are either under diffusion or kinetic control.[60] Future studies of catalysis with hydrophobic materials that can determine whether measured rates reflect diffusion or kinetic control, by using accepted assessments of transport contributions (e.g., Koros-Nowak or Madon-Boudart criteria)[85], will be able to guide efforts that functionalize external or internal surfaces in porous solids, as appropriate, to cause informed and desired changes in reactivity.

The structural degradation of crystalline and mesoporous silicates in the presence of water occurs by different mechanisms in the vapor and liquid phases. In liquid phases, the hydrolysis of framework Si-O-Si connectivities,[42, 48] Si-O-Al connectivities,[46, 47] and organic functional groups[58] are common degradation mechanisms. These hydrolysis events can be mitigated either by making internal or external oxide surfaces more hydrophobic, which prevent liquid water from facilitating transport and removal of soluble framework species into bulk solution.[49] Although theory predicts that extended water phases are not stable (at ambient conditions) between flat hydrophobic surfaces separated by less than one nanometer,[29, 30] void spaces in low-defect pure-silica microporous materials (<1 nm in diameter, Figure 1)[15] and mesoporous MCM-41 (<3 nm in diameter)[86] display hydrophobic properties, reflected in order of magnitude lower uptakes for water than for nitrogen or organic molecules in single-component vapor isotherms. Mesoporous silicas containing low-defect surfaces in the vicinity of active sites could increase reaction rates by mitigating competitive inhibition by water adsorption and by improving the resistance of these sites to hydrolysis. Yet, it is plausible that much larger pores (>3 nm in diameter)[86] can condense bulk water within them, and therefore may influence

reaction rates limited by molecular transport. Further research to determine the effects of pore size and defect density on hydrophobicity can provide specific guidance for the design of hydrophobic mesopores with size ranges that can accommodate biomass-derived molecules that are too large to react within microporous voids.

Several options are available to design microporous and mesoporous oxides with hydrophobic properties during and after synthesis.[81] The use of fluoride anions as mineralizers for silica species during cation-directed zeolite synthesis can limit the number of defective silanol groups formed, as has been shown for purely siliceous[87] and Brønsted acidic aluminosilicate MFI zeolites,[88] and for Lewis acidic metallosilicate BEA zeolites.[27] Another option to modify the internal hydrophobicity and effective pore sizes of mesoporous silicas is to functionalize defect surface groups with non-polar organic moieties,[72, 78-80, 89, 90] although these functional groups may compromise the thermal and hydrothermal stability of the material. Grafting reactions may also occur non-selectively with Brønsted and Lewis acidic active site structures instead of their surroundings.[48, 49, 82] Expanding the range of synthetic and post-synthetic tools that can tailor the hydrophobicity of oxide surfaces, while avoiding modification of active site structures, will likely open new opportunities for catalysis in liquid media, as occurred with the advent of hydrophobic TS-1 in the 1980s for hydrocarbon oxidation reactions in liquid water.

The modification of porous oxides can occur at internal voids and external crystal surfaces, each with fundamentally different consequences for the reactivity and stability of active sites contained within these oxides, but often with similar effects on observed reaction rates. A more rigorous assessment of how transport and reaction rates influence the reactivity of heterogeneous oxides in liquid media would provide insight into whether hydrophobic

environments at external or internal crystallite surfaces are catalytically-relevant for a given process or application. These insights, in turn, can guide efforts to design solid Brønsted and Lewis acids compatible with catalytic processing in liquid water or other solvents, a technical challenge relevant in the upgrading of chemical intermediates derived from the pyrolysis or hydrolysis of lignocellulosic biomass.

Acknowledgements

This work was supported as part of the Institute for Atom-Efficient Chemical Transformations (IACT), an Energy Frontier Research Center funded by the U.S. Department of Energy, Office of Science, Office of Basic Energy Sciences.

Tables

Table 1. Conversion for *n*-octane oxidation (373 K) and 1-hexene epoxidation (353 K) in anhydrous H_2O_2 (methyl ethyl ketone) and aqueous H_2O_2, and rate constants for glucose isomerization (373 K) in liquid water, measured on hydrophobic Ti-zeolites and hydrophilic TiO_2-SiO_2. The ratio of conversions or rate constants on the two catalysts is also shown.

Reaction	Solvent	Catalyst		
		Hydrophobic Ti-zeolite	Hydrophilic TiO_2-SiO_2	Ratio of Ti-zeolite/ TiO_2-SiO_2
		Conversion (%)		
n-Octane oxidation[a]	Methyl ethyl ketone	16	2.71	6
n-Octane oxidation[a]	Water	15	0.14	100
1-Hexene epoxidation[a]	Methyl ethyl ketone	8	1.86	4
1-Hexene epoxidation[a]	Water	7	0.24	29
		First-order rate constant[c]		
Glucose isomerization[b]	Water	26	0.91	28

[a]Data and experimental details reported in Khouw et al.[65] The hydrophobic Ti-zeolite used was Ti-MFI.
[b]Data and experimental details reported in Gounder et al.[70] The hydrophobic Ti-zeolite used was Ti-BEA.
[c]Units of measured first-order rate constant are ($/10^{-6}$ mol (mol Ti*s*(mol(glucose) m^{-3}))$^{-1}$)).

Table 2. Conversion for glucose isomerization and selectivity to fructose in liquid water (413 K), measured on Lewis acid zeolites and mesoporous materials.

Catalyst	Glucose conversion[a] (%)	Selectivity to fructose (%)
Ti-Beta	50	44
Ti-MCM-41	22	26
Sn-Beta	82	28
Sn-MCM-41	30	40

[a]Data and experimental details reported in Moliner et al.[67] 50:1 glucose:metal ratio. Supra-equilibrium glucose conversions reflect fructose degradation side reactions that required additional glucose conversion to re-establish equilibrium.

Figures and Schemes

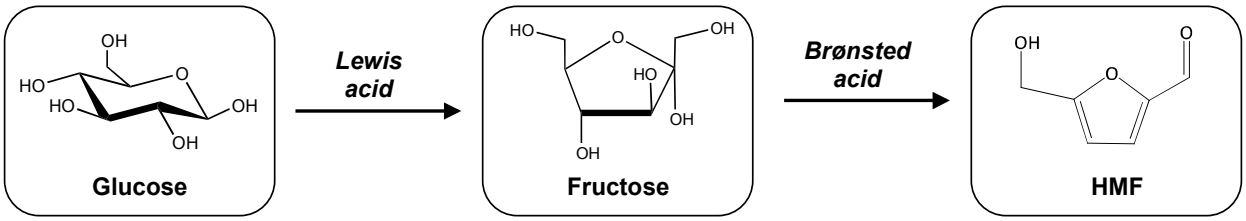

Scheme 1. Reaction scheme for sequential Lewis acid-catalyzed glucose isomerization to fructose and Brønsted acid-catalyzed fructose dehydration to 5-hydroxymethylfurfural (HMF).

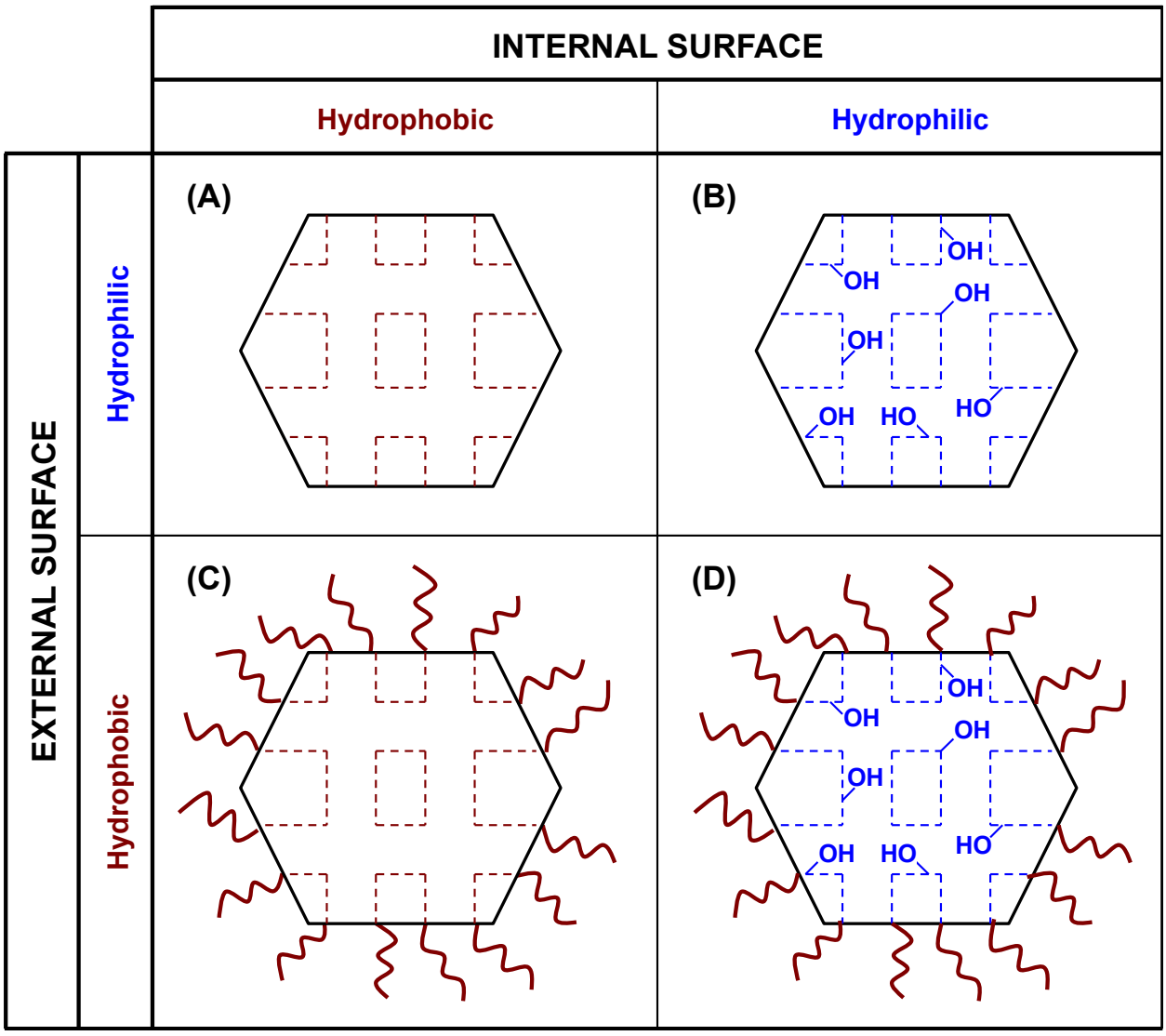

Scheme 2. Schematic depiction of zeolite crystals with hydrophobic (red) or hydrophilic (blue) domains located at external crystal surfaces (solid lines) or internal pore surfaces (dashed lines).

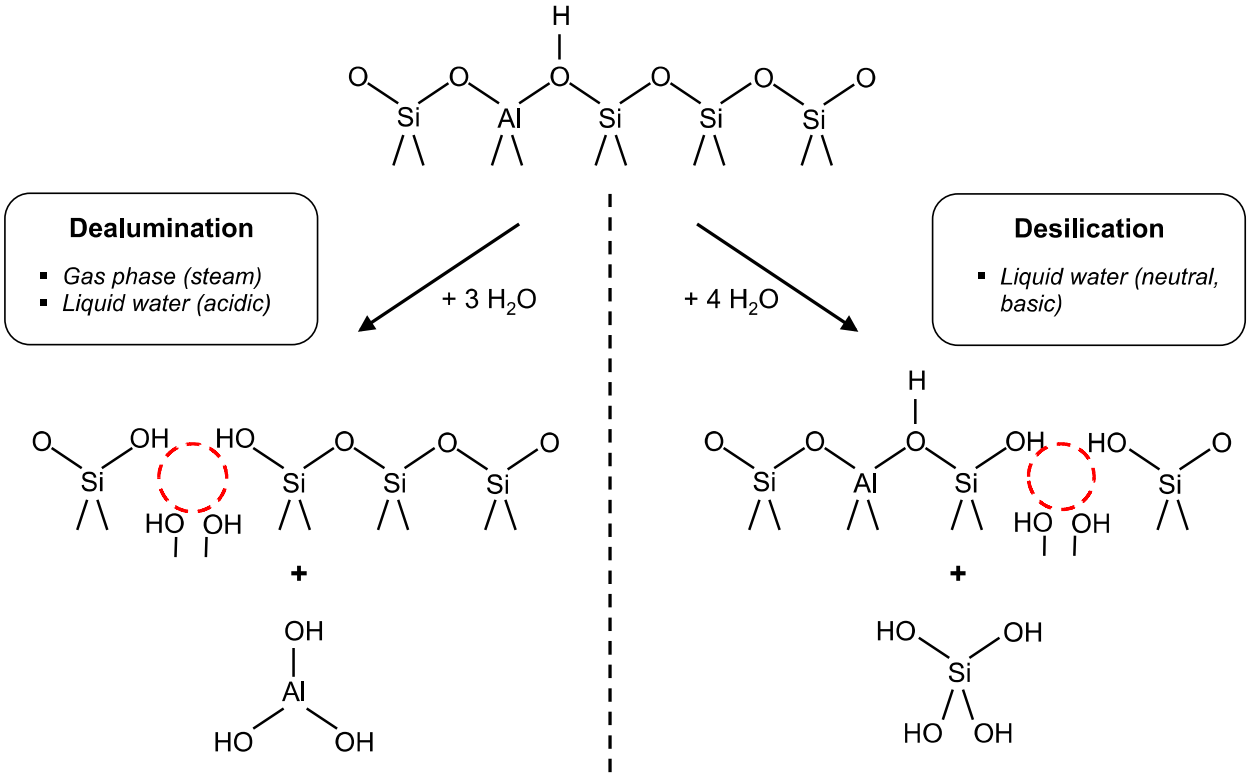

Scheme 3. Hydrolysis reactions that lead to framework dealumination (left) prevail in the gas phase with steam and in liquid water under acidic conditions. Hydrolysis reactions that lead to framework desilication (right) prevail in liquid water under neutral and basic conditions.

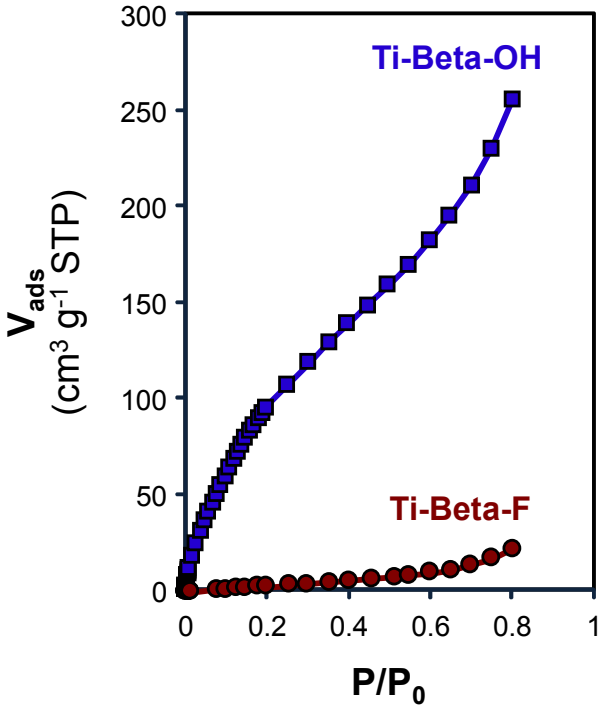

Figure 1. Water adsorption isotherms (293 K) on low-defect Ti-Beta zeolites crystallized in fluoride media (Ti-Beta-F, red circles) and on highly defective Ti-Beta zeolites crystallized in hydroxide media (Ti-Beta-OH, blue squares). The surface properties of Ti-Beta-F and Ti-Beta-OH are depicted by the structures in Schemes 2a and 2b, respectively. Figure adapted from data reported in Gounder and Davis.[15]

References

1. J. N. Chheda, G. W. Huber and J. A. Dumesic, *Angew. Chem., Int. Ed.*, 2007, 46, 7164-7183.
2. G. W. Huber, S. Iborra and A. Corma, *Chem. Rev.*, 2006, 106, 4044-4098.
3. L. Bui, H. Luo, W. R. Gunther and Y. Roman-Leshkov, *Angew. Chem., Int. Ed.*, 2013, 52, 8022-8025.
4. M. J. Climent, A. Corma, S. Iborra and M. J. Sabater, *ACS Catal.*, 2014, 4, 870-891.
5. M. Moliner, *Dalton Trans.*, 2014, 43, 4197-4208.
6. M. Dusselier, M. Mascal and B. F. Sels, Springer Berlin Heidelberg, 2014, ch. 544, pp. 1-40.
7. E. Nikolla, Y. Román-Leshkov, M. Moliner and M. E. Davis, *ACS Catal.*, 2011, 1, 408-410.
8. D. M. Alonso, S. G. Wettstein, J. Q. Bond, T. W. Root and J. A. Dumesic, *ChemSusChem*, 2011, 4, 1078-1081.
9. E. I. Gurbuz, S. G. Wettstein and J. A. Dumesic, *ChemSusChem*, 2012, 5, 383-387.
10. J. S. Luterbacher, J. M. Rand, D. M. Alonso, J. Han, J. T. Youngquist, C. T. Maravelias, B. F. Pfleger and J. A. Dumesic, *Science*, 2014, 343, 277-280.
11. J. M. R. Gallo, D. M. Alonso, M. A. Mellmer, J. H. Yeap, H. C. Wong and J. A. Dumesic, *Top. Catal.*, 2013, 56, 1775-1781.
12. E. I. Gurbuz, J. M. R. Gallo, D. M. Alonso, S. G. Wettstein, W. Y. Lim and J. A. Dumesic, *Angew. Chem., Int. Ed.*, 2013, 52, 1270-1274.
13. C. Sievers, I. Musin, T. Marzialetti, M. B. V. Olarte, P. K. Agrawal and C. W. Jones, *ChemSusChem*, 2009, 2, 665-671.
14. H. B. Zhao, J. E. Holladay, H. Brown and Z. C. Zhang, *Science*, 2007, 316, 1597-1600.
15. R. Gounder and M. E. Davis, *AIChE J.*, 2013, 59, 3349-3358.
16. M. E. Davis, *Chem. Mater.*, 2014, 26, 239-245.
17. Y. Roman-Leshkov and M. E. Davis, *ACS Catal.*, 2011, 1, 1566-1580.
18. A. Corma, *Chem. Rev.*, 1995, 95, 559-614.
19. M. E. Davis, *Acc. Chem. Res.*, 1993, 26, 111-115.
20. A. Corma, *Chem. Rev.*, 1997, 97, 2373-2419.
21. M. E. Davis, *Nature*, 2002, 417, 813-821.
22. A. Taguchi and F. Schuth, *Microporous Mesoporous Mater.*, 2005, 77, 1-45.
23. T. Okuhara, *Chem. Rev.*, 2002, 102, 3641-3665.
24. G. J. Young, *J. Colloid Sci.*, 1958, 13, 67-85.
25. N. Y. Chen, *J. Phys. Chem.*, 1976, 80, 60-64.
26. X. S. Zhao, G. Q. Lu, A. K. Whittaker, G. J. Millar and H. Y. Zhu, *J. Phys. Chem. B*, 1997, 101, 6525-6531.
27. T. Blasco, M. A. Camblor, A. Corma, P. Esteve, J. M. Guil, A. Martinez, J. A. Perdigon-Melon and S. Valencia, *J. Phys. Chem. B*, 1998, 102, 75-88.
28. R. Bermejo-Deval, R. S. Assary, E. Nikolla, M. Moliner, Y. Román-Leshkov, S.-J. Hwang, A. Pallsdottir, D. Silverman, R. F. Lobo, L. A. Curtiss and M. E. Davis, *Proc. Natl. Acad. Sci. USA*, 2012, 109, 9727-9732.
29. N. Giovambattista, P. J. Rossky and P. G. Debenedetti, *Phys. Rev. E*, 2006, 73, 041604.
30. N. Giovambattista, P. G. Debenedetti and P. J. Rossky, *J. Phys. Chem. C*, 2007, 111, 1323-1332.

31. B. Rotenberg, A. J. Patel and D. Chandler, *J. Am. Chem. Soc.*, 2011, 133, 20521-20527.
32. P. Bai, J. I. Siepmann and M. W. Deem, *AIChE J.*, 2013, 59, 3253-3259.
33. P. B. Venuto, *Microporous Mater.*, 1994, 2, 297-411.
34. W. Vermeiren and J. P. Gilson, *Top. Catal.*, 2009, 52, 1131-1161.
35. G. T. Kerr, *J. Phys. Chem.*, 1967, 71, 4155-4156.
36. G. T. Kerr, *J. Catal.*, 1969, 15, 200-204.
37. R. Rinaldi and F. Schuth, *Energy Environ. Sci.*, 2009, 2, 610-626.
38. T. N. Pham, D. C. Shi and D. E. Resasco, *Appl. Catal. B*, 2014, 145, 10-23.
39. R. T. Carr, M. Neurock and E. Iglesia, *J. Catal.*, 2011, 278, 78-93.
40. R. Gounder, A. J. Jones, R. T. Carr and E. Iglesia, *J. Catal.*, 2012, 286, 214-223.
41. A. J. Jones, R. T. Carr, S. I. Zones and E. Iglesia, *J. Catal.*, 2014, 312, 58-68.
42. H. Chiang and A. Bhan, *J. Catal.*, 2010, 271, 251-261.
43. J. Macht, R. T. Carr and E. Iglesia, *J. Catal.*, 2009, 264, 54-66.
44. R. M. West, D. J. Braden and J. A. Dumesic, *J. Catal.*, 2009, 262, 134-143.
45. R. M. Ravenelle, F. Schussler, A. D'Amico, N. Danilina, J. A. van Bokhoven, J. A. Lercher, C. W. Jones and C. Sievers, *J. Phys. Chem. C*, 2010, 114, 19582-19595.
46. J. S. Kruger, V. Choudhary, V. Nikolakis and D. G. Vlachos, *ACS Catal.*, 2013, 3, 1279-1291.
47. J. S. Kruger, V. Nikolakis and D. G. Vlachos, *Appl. Catal. A*, 2014, 469, 116-123.
48. P. A. Zapata, J. Faria, M. P. Ruiz, R. E. Jentoft and D. E. Resasco, *J. Am. Chem. Soc.*, 2012, 134, 8570-8578.
49. P. A. Zapata, Y. Huang, M. A. Gonzalez-Borja and D. E. Resasco, *J. Catal.*, 2013, 308, 82-97.
50. S. I. Zones, *J. Chem. Soc. Faraday Trans.*, 1991, 87, 3709-3716.
51. R. A. Pollock, G. Y. Gor, B. R. Walsh, J. Fry, I. T. Ghampson, Y. B. Melnichenko, H. Kaiser, W. J. DeSisto, M. C. Wheeler and B. G. Frederick, *J. Phys. Chem. C*, 2012, 116, 22802-22814.
52. J. M. Kim and R. Ryoo, *Bull. Korean Chem. Soc.*, 1996, 17, 66-68.
53. R. Mokaya, *J. Phys. Chem. B*, 2000, 104, 8279-8286.
54. S. C. Shen and S. Kawi, *J. Phys. Chem. B*, 1999, 103, 8870-8876.
55. Y. D. Xia and R. Mokaya, *J. Phys. Chem. B*, 2003, 107, 6954-6960.
56. Q. H. Yang, J. Liu, L. Zhang and C. Li, *J. Mater. Chem.*, 2009, 19, 1945-1955.
57. M. C. Burleigh, M. A. Markowitz, S. Jayasundera, M. S. Spector, C. W. Thomas and B. P. Gaber, *J. Phys. Chem. B*, 2003, 107, 12628-12634.
58. A. J. Crisci, M. H. Tucker, J. A. Dumesic and S. L. Scott, *Top. Catal.*, 2010, 53, 1185-1192.
59. M. H. Tucker, A. J. Crisci, B. N. Wigington, N. Phadke, R. Alamillo, J. P. Zhang, S. L. Scott and J. A. Dumesic, *ACS Catal.*, 2012, 2, 1865-1876.
60. R. J. Madon and E. Iglesia, *J. Mol. Catal. A*, 2000, 163, 189-204.
61. M. A. Camblor, A. Corma, S. Iborra, S. Miquel, J. Primo and S. Valencia, *J. Catal.*, 1997, 172, 76-84.
62. K. S. Arias, M. J. Climent, A. Corma and S. Iborra, *ChemSusChem*, 2014, 7, 210-220.
63. G. Perego, G. Bellussi, C. Corno, M. Taramasso, F. Buonomo and A. Esposito, in *New Developments in Zeolite Science and Technology, Proceedings of the 7th International Zeolite Conference*, Elsevier Science Publ B V, Tokyo, 1986, vol. 28, pp. 129-136.
64. M. Taramasso, G. Perego and B. Notari, *U. S. Pat.,* 4,410,501, 1983.

65. C. B. Khouw, C. B. Dartt, J. A. Labinger and M. E. Davis, *J. Catal.*, 1994, 149, 195-205.
66. B. Notari, in *Advances in Catalysis, Vol 41*, Elsevier Academic Press Inc, San Diego, 1996, vol. 41, pp. 253-334.
67. M. Moliner, Y. Román-Leshkov and M. E. Davis, *Proc. Natl. Acad. Sci. U. S. A.*, 2010, 107, 6164-6168.
68. V. Choudhary, A. B. Pinar, S. I. Sandler, D. G. Vlachos and R. F. Lobo, *ACS Catal.*, 2011, 1, 1724-1728.
69. Y. Román-Leshkov, M. Moliner, J. A. Labinger and M. E. Davis, *Angew. Chem., Int. Ed.*, 2010, 49, 8954-8957.
70. R. Gounder and M. E. Davis, *J. Catal.*, 2013, 308, 176-188.
71. A. Corma, M. E. Domine and S. Valencia, *J. Catal.*, 2003, 215, 294-304.
72. R. Alamillo, A. J. Crisci, J. M. R. Gallo, S. L. Scott and J. A. Dumesic, *Angew. Chem., Int. Ed.*, 2013, 52, 10349-10351.
73. A. J. Crisci, M. H. Tucker, M. Y. Lee, S. G. Jang, J. A. Dumesic and S. L. Scott, *ACS Catal.*, 2011, 1, 719-728.
74. S. J. Miao and B. H. Shanks, *J. Catal.*, 2011, 279, 136-143.
75. S. J. Miao and B. H. Shanks, *Appl. Catal. A*, 2009, 359, 113-120.
76. I. K. Mbaraka and B. H. Shanks, *J. Catal.*, 2006, 244, 78-85.
77. P. Y. Dapsens, C. Mondelli, J. Jagielski, R. Hauert and J. Perez-Ramirez, *Catal. Sci. Technol.*, 2014.
78. A. Corma, M. Domine, J. A. Gaona, J. L. Jorda, M. T. Navarro, F. Rey, J. Perez-Pariente, J. Tsuji, B. McCulloch and L. T. Nemeth, *Chem. Commun.*, 1998, 2211-2212.
79. K. A. Koyano, T. Tatsumi, Y. Tanaka and S. Nakata, *J. Phys. Chem. B*, 1997, 101, 9436-9440.
80. T. Tatsumi, K. A. Koyano and N. Igarashi, *Chem. Commun.*, 1998, 325-326.
81. M. Moliner and A. Corma, *Microporous Mesoporous Mater.*, 2014, 189, 31-40.
82. T. Kamegawa, N. Suzuki, K. Tsuji, J. Sonoda, Y. Kuwahara, K. Mori and H. Yamashita, *Catal. Today*, 2011, 175, 393-397.
83. L. Li, T. I. Koranyi, B. F. Sels and P. P. Pescarmona, *Green Chem.*, 2012, 14, 1611-1619.
84. C. X. A. da Silva, V. L. C. Goncalves and C. J. A. Mota, *Green Chem.*, 2009, 11, 38-41.
85. R. J. Davis, in *Catalysis for the Conversion of Biomass and Its Derivatives*, eds. M. Behrens and A. K. Datye, epubli GmbH, Berlin, 2013, ch. 9, pp. 255-291.
86. C. Y. Chen, H. X. Li and M. E. Davis, *Microporous Mater.*, 1993, 2, 17-26.
87. E. E. Mallon, M. Y. Jeon, M. Navarro, A. Bhan and M. Tsapatsis, *Langmuir*, 2013, 29, 6546-6555.
88. Z. X. Qin, L. Lakiss, L. Tosheva, J. P. Gilson, A. Vicente, C. Fernandez and V. Valtchev, *Adv. Funct. Mater.*, 2014, 24, 257-264.
89. V. Valtchev, G. Majano, S. Mintova and J. Perez-Ramirez, *Chem. Soc. Rev.*, 2013, 42, 263-290.
90. F. de Clippel, M. Dusselier, S. Van de Vyver, L. Peng, P. A. Jacobs and B. F. Sels, *Green. Chem.*, 2013, 15, 1398-1430.